



OPEN Genome-wide analysis of the *KCS* gene family in *Medicago truncatula* and their expression profile under various abiotic stress

Peng Lv^{1,4}, Jiaqi Lv^{1,4}, Yawen Zhan¹, Ning Wang², Xinyan Zhao¹, Qi Sha¹, Wen Zhou¹, Yujie Gong¹, Jing Yang¹, Hang Zhou³, Pengfei Chu^{1✉} & Yongwang Sun^{1✉}

Very long-chain fatty acids (VLCFAs) are indispensable constituents of cuticular wax and exert pivotal functions in regulating plant growth, development and response to stress. β -Ketoacyl-CoA synthase (KCS) represents the rate-limiting enzyme for the biosynthesis of VLCFAs. In this study, 25 *KCS* genes were identified in the *M. truncatula* genome and were unevenly distributed across seven of the eight chromosomes. The 25 *MtKCS* genes were clustered into seven groups, each exhibiting conserved gene structure and motif distribution. *MtKCS* gene promoters contained multiple hormone signaling and stress-responsive elements, indicating that the expression of these genes may be modulated by a range of developmental and environmental stimuli. The expression profiles revealed that the *MtKCS* genes exhibit diverse expression patterns across various organs/tissues and are differentially expressed under abiotic stress. It is noteworthy that several genes, such as *MtKCS2*, *10*, and *13*, exhibited significantly increased expression in leaves under cold, heat, salt, and drought stress. This suggests that *MtKCS* genes may play an integral role in the abiotic stress resistance of *M. truncatula*. These findings establish a foundation for understanding the evolution of *KCS* genes in higher plants and facilitated further functional exploration of *MtKCS* genes.

Keywords Very long chain fatty acids, β -Ketoacyl-CoA synthase, Gene family, *Medicago truncatula*, Abiotic stress, Expression profile

As sessile organisms, plants are persistently confronted with a multitude of detrimental factors that impede their growth and, in some cases, even their survival. These factors can be broadly classified into two categories: biotic stresses, which originate from other living organisms, and abiotic stresses, which are caused by non-living environmental factors^{1,2}. In order to mitigate the effects of adverse conditions, plants have evolved a variety of protective mechanisms, among which cuticular wax plays an important role in their defence process^{3,4}. Cuticular wax is a protective substance that covers the aerial parts of all terrestrial plants, forming the interface between plants and their environment^{5,6}. It fulfils a number of biological functions, including the prevention of non-stomatal water loss and the provision of a protective barrier against adverse factors such as insects, pathogens, physical friction and UV radiation^{7,8}.

Very long-chain fatty acids (VLCFAs) are defined as fatty acids with a hydrocarbon chain of 20 or more carbon atoms. They serve as the primary building block for cuticular waxes and numerous other lipids, including triacylglycerols accumulated in seeds, as well as some sphingolipids and phospholipids in cell membranes^{9,10}. The biosynthesis of VLCFAs commences with C18 in the plastid, which is subsequently catalyzed by the long-chain fatty acid acyl-CoA elongase (FAE) multiprotein complex in the endoplasmic reticulum¹¹. The FAE complex is composed of four different enzymes, namely β -Ketoacyl-CoA synthetase (KCS), β -Ketoacyl-CoA reductase (KCR), β -Hydroxyacyl-CoA dehydratase (HCD), and β -Enoyl-CoA reductase (ECR), which catalyze four successive reactions including condensation, reduction, dehydration, and second reduction, respectively^{12,13}. The substrate and tissue specificity exhibited by different KCS isoforms determine the synthesis rate and carbon chain length of VLCFAs. In contrast, the other three enzymes have broad substrate catalytic properties and are shared by all FAE complexes¹⁴. Consequently, KCS is the rate-limiting enzyme in the elongation process of

¹College of Agriculture and Biology, Liaocheng University, Liaocheng 252000, China. ²Rural Economic Development Center of Dong'e County, Liaocheng 252000, China. ³Shennong Zhiyi Intelligent Technology Co., Ltd, Liaocheng 252000, China. ⁴Peng Lv and Jiaqi Lv contributed equally to this work. ✉email: chupengfei@lcu.edu.cn; sunyongwang@lcu.edu.cn

VLCFAs and is responsible for the composition and content of cuticular waxes, thereby influencing the capability of plants to resist stress^{9,15}.

FAE1/AtKCS18 is the first KCS gene cloned and characterized in higher plants. It was found to be specifically expressed in developing seeds in *Arabidopsis thaliana*, where it catalyzes the synthesis of C18:1 to C20:1, C20:1 to C22:1, and C18:0 to C20:0 fatty acids for lipid storage¹⁶. Overexpression of the *FAE1/AtKCS18* in *Arabidopsis* and rapeseed (*Brassica napus*) resulted in a notable increase in erucic acid (C22:1) content^{17,18}. KCSs are characterized by the presence of two conserved structural domains: the FAE1/Type III polyketide synthase-like protein domain (FAE1_CUT1_RppA) and the 3-Oxoacyl- [acyl-carrier-protein (ACP)] synthase III C-terminal domain (ACP_syn_III_C)¹⁹. The former comprises the motif that specifically binds to the substrate, which may be related to substrate specificity²⁰. The KCS gene family in *Arabidopsis* has been the subject of the most comprehensive study and characterization in terms of its physiological and molecular functions. Based on their phylogenetic relationship and duplication history, 21 *AtKCS* genes can be categorized into eight subclasses (α , β , γ , δ , ϵ , ζ , η , and θ)²¹. Functional studies have confirmed that *AtKCS* genes play crucial roles in the biosynthesis of epidermal wax^{22–26}, root suberin metabolism^{27–29}, seed stored triglycerides¹⁶, maintenance of leaf guard cell density³⁰, and development of the epidermis³¹.

The genome-wide identification of a gene family will substantially facilitate the investigation of gene function. Given their pivotal role in plant growth, development, and stress responses^{9,32,33}, KCS gene families have been identified in dozens of plant species, exhibiting notable variation in the type and quantity of these genes across different species. For example, 22 in rice (*Oryza sativa*)³³, 24 in grape (*Vitis vinifera*)³⁴, 25 in sorghum (*Sorghum bicolor*)³⁵, 26 in maize (*Zea mays*)³⁶, 28 in apple (*Malus × domestica* Borkh.)³⁷, 31 in soybean (*Glycine max*)³⁸, 35 in pear (*Pyrus bretschneideri*)³⁹, and as many as 58 in upland cotton (*Gossypium hirsutum*)⁴⁰ and rapeseed⁴¹.

A substantial body of research has demonstrated that the KCS family genes play a pivotal role in determining the composition and structure of epidermal wax, actively engage in physiological and biochemical processes throughout the entire life cycle of plants, and are instrumental in shaping their stress resistance. For example, *AtKCS1* has been demonstrated to regulate the biosynthesis of C26–C30 wax alcohols and aldehydes. Compared with wild type, the *Atkcs1* mutant displayed a reduction in seedling growth under conditions of drought, low humidity, and chilling tolerance^{22,42}. *AtKCS4* plays a crucial role in regulating lipid metabolism in response to heat and dark conditions³². HMS1 has been demonstrated to catalyze the biosynthesis of the C26 and C28 VLCFAs in rice, contributing to the formation of bacula and tryphine in the pollen wall, which protect the pollen from low humidity⁴². The overexpression of *GhKCS13* in transgenic cotton plants resulted in enhanced sensitivity to cold stress, which was attributed to the modulation of lipid and oxylipin biosynthesis⁴³. The ectopic expression of *VvKCS11* from grape or *CcKCS6* from navel orange (*Citrus clementina*) in transgenic *Arabidopsis* plants resulted in enhanced tolerance to various abiotic stresses^{44,45}. In alfalfa (*Medicago sativa*), *MsKCS10* exhibited high expression levels in leaves and was markedly induced by drought stress. Subsequent experiments demonstrated that it regulated wax biosynthesis and wax crystal morphology, thereby positively influencing the plant's drought stress response⁴⁶.

The Leguminosae family represents the third largest group of flowering plants, comprising a diverse range of food and forage crops. Notable examples of food crops include soybeans, peanuts, peas, chickpeas, and lentils, while forage crops include alfalfa and clover. It is one of the most economically significant plant groups, ranking second only to the Gramineae family⁴⁷. The diploid plant *Medicago truncatula*, with its relatively small genome (approximately 465 Mb), short life cycle, self-fertility, and high genetic transformation efficiency, has been selected as an exemplary model species for legume genetic research and functional genomic research⁴⁸. Two *MtKCS* genes have been the subject of functional exploration, with the findings indicating their involvement in lateral organ development and cuticular wax synthesis⁴⁹, as well as the preservation of seed physical dormancy through the regulation of VLCFA production in the seed coat⁵⁰. However, a comprehensive and systematic exploration of the KCS gene family in *M. truncatula* has yet to be conducted.

This study aims to characterize the KCS gene family in *M. truncatula* using bioinformatic methods. A total of 25 *MtKCS* genes were identified, and their chromosomal distribution, gene structure, conserved motif distribution, gene synteny, and phylogenetic relationships were analyzed. To gain further insight into the potential functions of the *MtKCS* genes, their tissue-specific expression profiles and response patterns to cold, heat, salt, and drought stresses were examined. These findings provide a foundation for comprehending the roles of the *MtKCS* gene family and offer valuable insights into how these genes contribute to stress tolerance mechanisms in *M. truncatula*.

Results

Identification of *MtKCS* genes and characterization of their protein physicochemical properties

A total of 25 sequences in the *M. truncatula* protein database were found to contain both the ACP_syn_III_C and FAE1_CUT1_RppA domains, and they were considered as members of the *MtKCS* gene family. The corresponding genes were named as *MtKCS1* to *MtKCS25* in accordance with their chromosomal positions (Table 1; Fig. 1A), with the nucleotide sequence lengths varying from 690 bp (*MtKCS14*) to 3348 bp (*MtKCS13*). Moreover, the physicochemical properties of the *MtKCS* proteins were examined. *MtKCS14* and *MtKCS25* were the shortest and longest proteins, with 229 and 534 amino acid residues, respectively. The molecular weight of the *MtKCS* proteins ranged from 25.90 kDa (*MtKCS14*) to 60.67 kDa (*MtKCS13*), while the theoretical isoelectric points varied from 8.50 (*MtKCS21*) to 9.35 (*MtKCS9* and *MtKCS23*). These findings suggest that all *MtKCS* proteins tend to be weakly basic. The instability index demonstrated that twelve proteins exhibited potential instability (>40), whereas the remaining proteins demonstrated stability (ranging from 25.90 to 39.09). The aliphatic index, which ranged from 83.80 (*MtKCS14*) to 103.22 (*MtKCS6*), indicated that the proteins were

Name	Gene ID	Chromosomal location	Gene length (bp)	Protein length (aa)	MW (kDa)	Isoelectric point	Instability index	Aliphatic index	GRAVY
MtKCS1	MtrunA17_Chr1g0166191	Chr1:15596128–15,599,422	3294	521	58.94	9.34	38.45	95.41	−0.051
MtKCS2	MtrunA17_Chr1g0188051	Chr1:37903862–37,906,011	2149	516	58.09	8.99	39.09	90.72	−0.102
MtKCS3	MtrunA17_Chr1g0204301	Chr1:49833353–49,834,816	1463	487	54.96	8.59	42.01	96.06	0.077
MtKCS4	MtrunA17_Chr1g0209881	Chr1:53778029–53,776,539	1490	496	55.96	9.19	40.83	99.64	0.005
MtKCS5	MtrunA17_Chr1g0212951	Chr1:55951743–55,953,197	1454	484	55.39	8.76	35.13	88.80	−0.085
MtKCS6	MtrunA17_Chr2g0277841	Chr2:801797–803,167	1370	456	51.07	8.70	34.64	103.22	0.092
MtKCS7	MtrunA17_Chr2g0282281	Chr2:3753581–3,756,082	2501	505	57.15	9.10	36.09	92.65	−0.168
MtKCS8	MtrunA17_Chr2g0295781	Chr2:14181817–14,183,184	1367	455	51.37	9.17	44.44	91.08	−0.021
MtKCS9	MtrunA17_Chr2g0306781	Chr2:28895040–28,896,575	1535	405	45.25	9.35	33.35	89.11	−0.205
MtKCS10	MtrunA17_Chr2g0327721	Chr2:47186905–47,185,463	1442	480	54.46	8.85	44.92	90.40	−0.178
MtKCS11	MtrunA17_Chr3g0115021	Chr3:36326838–36,325,375	1463	487	54.83	8.71	47.83	93.31	0.010
MtKCS12	MtrunA17_Chr3g0115041	Chr3:36340115–36,338,652	1463	487	54.86	8.71	48.08	48.08	0.005
MtKCS13	MtrunA17_Chr3g0136561	Chr3:48669145–48,672,493	3348	537	60.67	8.91	42.24	84.60	−0.189
MtKCS14	MtrunA17_Chr4g0026871	Chr4:27836505–27,837,194	690	229	25.90	8.98	25.90	83.80	−0.185
MtKCS15	MtrunA17_Chr4g0030581	Chr4:31238302–31,236,884	1418	472	53.50	8.99	44.83	93.14	−0.159
MtKCS16	MtrunA17_Chr4g0030591	Chr4:31242909–31,241,488	1421	473	53.30	8.70	40.77	93.13	−0.106
MtKCS17	MtrunA17_Chr4g0030601	Chr4:31274362–31,275,756	1394	464	52.51	8.91	38.66	91.57	−0.149
MtKCS18	MtrunA17_Chr4g0035081	Chr4:34585407–34,586,921	1514	504	56.84	9.29	37.27	94.58	−0.052
MtKCS19	MtrunA17_Chr4g0063011	Chr4:54682129–54,683,631	1502	500	56.60	9.27	37.59	90.06	−0.117
MtKCS20	MtrunA17_Chr5g0423521	Chr5:25314651–25,313,161	1490	496	56.47	9.24	42.65	96.33	0.001
MtKCS21	MtrunA17_Chr6g0469631	Chr6:19384005–19,385,465	1460	486	54.74	8.50	48.19	99.28	0.094
MtKCS22	MtrunA17_Chr6g0480561	Chr6:35295872–35,293,613	2259	470	52.97	8.88	46.65	94.38	0.001
MtKCS23	MtrunA17_Chr7g0250661	Chr7:38096471–38,097,358	887	295	33.11	9.35	31.18	89.93	−0.184
MtKCS24	MtrunA17_Chr7g0276241	Chr7:55866823–55,867,710	887	295	33.00	8.71	32.49	77.02	−0.273
MtKCS25	MtrunA17_Chr7g0276251	Chr7:55869878–55,868,274	1604	534	59.84	8.98	34.05	94.01	−0.069

Table 1. Basic information of *MtKCS* genes and physicochemical properties of their protein sequences.

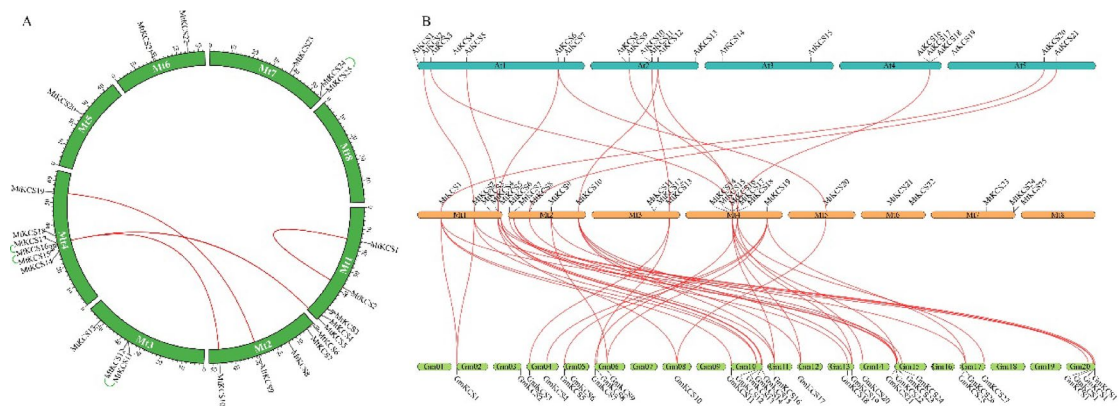


Fig. 1. Chromosomal location and the synteny relationships of *KCS* genes. (A) The segmental and tandem duplicated *MtKCS* genes are connected by red and green curves, respectively. (B) Synteny analysis of *KCS* genes between *M. truncatula* and *Arabidopsis*, and *M. truncatula* and soybean. The red curves indicate the synteny *KCS* gene pairs between different species.

thermally stable. The grand average of hydropathy index (GRAVY) exhibited a range from −0.27 (*MtKCS24*) to 0.09 (*MtKCS6*), indicating that these proteins possess amphoteric characteristics (Table 1).

Prediction of subcellular localization and transmembrane-spanning alpha-helix of *MtKCS* proteins

Subcellular localization prediction indicated that *MtKCS* proteins were predominantly localized in the plasma membrane, chloroplast, endoplasmic reticulum, cytoplasm, nucleus, and vacuole (Fig. S1). This suggests that they may be predominantly expressed and function in these organelles. It has been reported that *KCSs* are transmembrane proteins, with the transmembrane-spanning alpha-helix (TAH) being necessary for their

biological function⁵¹. The prediction of the TAH domains of MtKCS proteins indicated that thirteen proteins exhibited two TAHs, one protein demonstrated three TAHs, three proteins displayed a single TAH, and eight proteins lacked any TAHs (Fig. S2). The majority of TAH domains in MtKCS proteins are situated within the initial 100 amino acids of the N-terminus, with only a small proportion located towards the protein's central region.

Analyses of chromosomal distribution and synteny of *MtKCS* genes

The genomic distribution of *MtKCS* genes was determined by mapping their coding sequences onto the corresponding chromosomes. The distribution of *MtKCS* genes was found to be uneven across chromosomes 1–7, with no *MtKCS* present on chromosome 8. The greatest number of *MtKCS* genes was observed on chromosome 4 ($n=6$), followed by chromosomes 1 and 2 ($n=5$ each), and chromosomes 3 and 7 ($n=3$ each). Chromosomes 6 and 5 each contain two and one *MtKCS* gene, respectively (Fig. 1A). The expansion of gene families is primarily driven by segmental and tandem duplication⁵². Gene pairs located on the same chromosomes with a physical distance of less than 200 kb among them are generally considered to be tandemly duplicated, while those pairs localized on different chromosomes are termed as segmentally duplicated^{53,54}. To investigate gene duplication events within the *MtKCS* family, a collinearity analysis was conducted. A total of four segmentally duplicated gene pairs and four tandemly duplicated gene pairs were identified within the *MtKCS* gene family (Fig. 1A; Table 1). Moreover, a comparative syntenic analysis of *Arabidopsis* in conjunction with *M. truncatula* and of *M. truncatula* in conjunction with soybean was conducted to elucidate the evolutionary relationships of the KCS gene family among disparate species (Fig. 1B). A total of 12 and 36 orthologous pairs were identified between *Arabidopsis* and *M. truncatula*, and between *M. truncatula* and soybean, respectively. A collinear relationship was observed between nine *MtKCS* genes and those in *Arabidopsis*, with orthologous genes also present in soybean. This suggests that these genes may play an irreplaceable role in the evolution of the KCS gene family. In order to gain insight into the evolutionary selection pressure that shaped the formation of the KCS gene family, the K_a/K_s ratios of *MtKCS*-*MtKCS*, *MtKCS*-*AtKCS*, and *MtKCS*-*GmKCS* gene pairs were examined (Table S1). The K_a/K_s values for all gene pairs were found to be very low (0.02–0.24), indicating that strong purification selection pressure may have been exerted on KCS genes over the course of evolution.

Phylogenetic analysis and classification of *MtKCS* genes

In order to study the phylogenetic relationship and evolution of KCS genes in different plants, 157 KCS protein sequences from six diploid plants were used, including 21, 22, 25, 25, 31, and 33 from *Arabidopsis*, rice, *M. truncatula*, sorghum, soybean, and turnip (*Brassica rapa*), respectively. As illustrated in Fig. 2; Table 2, these KCS proteins were classified into nine groups, designated according to the *AtKCS* classification system²¹. It is noteworthy that group β is exclusive to two cruciferous plants: *Arabidopsis* and turnip. Groups α , γ , δ , ϵ , ζ , and θ are present in all six species, while groups λ and η are exclusive to monocotyledonous and dicotyledonous plants, respectively. *MtKCS*s were disproportionately distributed across seven groups, with the exception of groups β and λ . Group θ contained the highest number ($n=9$) of *MtKCS*s, followed by group ζ ($n=7$), γ , δ , ϵ and η ($n=2$ each), and α ($n=1$) (Fig. 2; Table 2).

Gene structure and conserved motif distribution of *MtKCS*s

The exon-intron arrangements of the *MtKCS* genes were analyzed using the coding sequence and DNA sequences of each gene. The *MtKCS* genes were found to be relatively simple, with a maximum of two introns. Of the 25 *MtKCS* genes analyzed, 19 (76%) exhibited no intron, while four genes (*MtKCS1*, 2, 9, and 22) from group ζ and two genes (*MtKCS7* and *MtKCS13*) from group ϵ had one intron and two introns, respectively (Fig. 3A,B). To identify potential functional diversification of *MtKCS* proteins, ten conserved motifs ranging in length from 21 to 50 amino acids were identified (Fig. 3C; Fig. S3). Motifs 1, 4, and 8 were identified in the C-terminus of all *MtKCS* proteins, with motifs 1 and 4 corresponding to the ACP_syn_III_C domain. Motifs 2, 3, 5, 6, 7, and 9 were found to correspond to the FAE1_CUT1_RppA domain. These motifs were identified in 21 *MtKCS* protein sequences. In contrast, the other four (*MtKCS9*, 14, 23, and 24) were found to contain a truncated FAE1_CUT1_RppA domain. No additional motifs were identified in members of groups η and θ . In contrast, motif 10 was observed in all members from groups α , γ , ϵ , and several members of groups ζ and δ , indicating that *MtKCS* family members possess a diverse N-terminus, which may be associated with their functional divergence.

Distribution of *cis*-acting elements in *MtKCS* gene promoters

In order to investigate the regulatory cues influencing gene expression, 2.0 kb of sequences located upstream of the start codon of the *MtKCS* genes were extracted and submitted to the PlantCARE website. A total of 19 *cis*-acting elements related to hormone and stress response were identified (Fig. 4). The number of abscisic acid responsive elements was the highest among the hormone-responsive elements (59), followed by ethylene-responsive (42), salicylic acid-responsive (31), methyl jasmonate-responsive (30), gibberellin-responsive (21), and auxin-responsive elements (10). *cis*-acting elements involved in ethylene and salicylic acid responsiveness were identified in the promoter regions of 21 and 20 *MtKCS* genes, respectively. All *MtKCS* promoters were found to contain at least one type of hormone-responsive element. Notably, the promoters of *MtKCS6* and *MtKCS17* were found to contain all of the aforementioned hormone-responsive elements. The *MtKCS* promoters were found to contain five distinct categories of stress-responsive elements. The most prevalent were the defense/stress elements (59), followed by anaerobic induction (53), wound- (37), drought- (20), and cold-response (12) elements. These elements were identified in 21, 23, 20, 17, and 10 *MtKCS* promoters, respectively. All *MtKCS* promoters exhibited the presence of at least two distinct types of stress-responsive elements. Notably, three promoters (*MtKCS3*, 13, and 16) demonstrated the co-occurrence of all five types of stress-responsive elements.

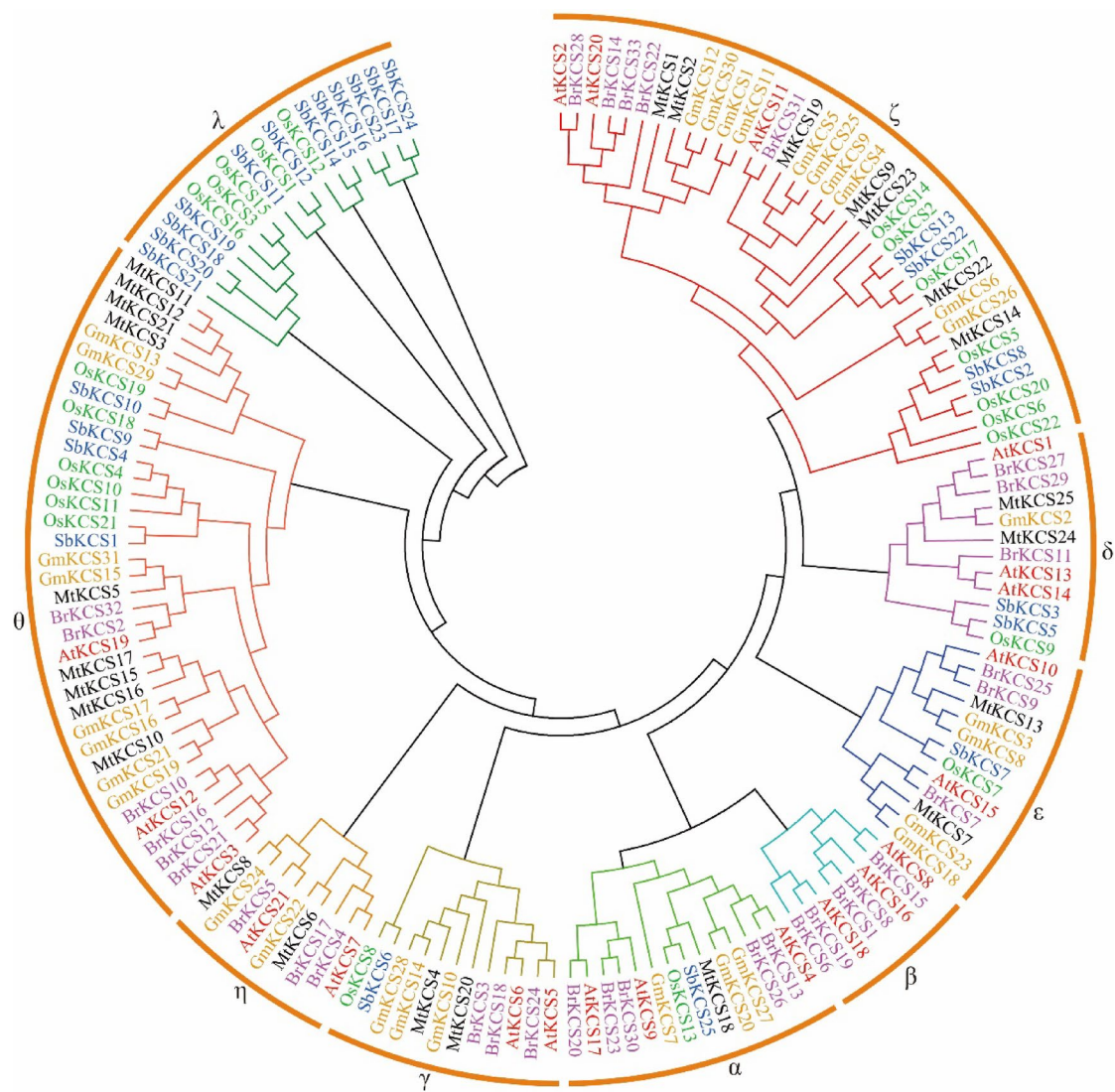


Fig. 2. Phylogenetic analysis of KCS proteins from six plant species. The protein sequences of 21 AtKCS, 22 OsKCS, 25 MtKCS, 25 SbKCS, 31 GmKCS, and 33 BrKCS were aligned using Clustal X software, and a neighbor-joining phylogenetic tree with 1000 bootstrap replicates was constructed using the MEGA 11.0 software.

Group	Arabidopsis	Turnip	M. truncatula	Soybean	Rice	Sorghum
α	3	5	1	3	1	1
β	3	5	0	0	0	0
γ	2	3	2	3	1	1
δ	3	3	2	1	1	2
ε	2	3	2	4	1	1
λ	0	0	0	0	5	12
ζ	3	5	7	10	7	4
η	2	3	2	2	0	0
θ	3	6	9	8	6	4

Table 2. The total number of KCS genes in each group of Arabidopsis, turnip, M. truncatula, soybean, rice and sorghum.



Fig. 3. Schematic diagrams of *MtKCS* genes and motif composition of *MtKCS* proteins. **(A)** A rootless neighbor-joining tree was constructed from the complete sequences of the 25 *MtKCS* proteins using MEGA11.0 software. **(B)** Structural analysis of the exon/intron distribution of the *MtKCS* genes, where the green boxes and black lines indicate the exons and introns, respectively. **(C)** Distribution map of conserved motifs in *MtKCS* proteins. The ten putative motifs are represented by different colored boxes. The length of the exon/intron junctions and the amino acid sequences are inferred from the ruler at the bottom.

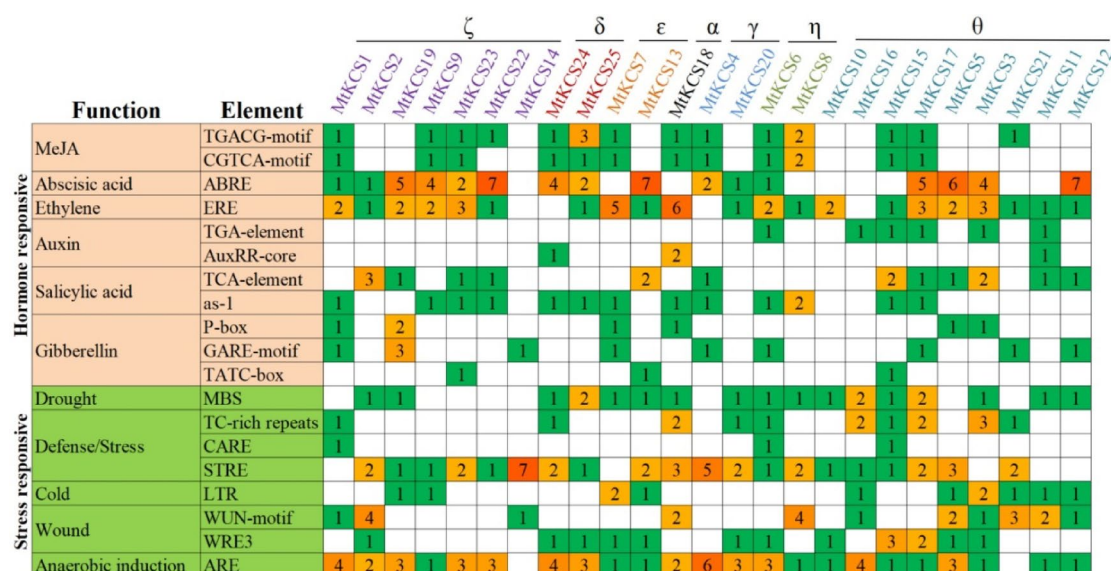


Fig. 4. Prediction of *cis*-acting elements in *MtKCS* promoters. Colors and numbers of the grid indicate the number of different *cis*-acting elements in *MtKCS* genes.

Expression profiles of *MtKCS* genes in different organs and developing seed tissues of *M. truncatula*

In order to gain insight into the expression patterns of *MtKCS* genes, the transcription levels of these genes in various *M. truncatula* tissues/organs, including roots, nodules, shoots, stems, leaves, flowers, developing embryos, endosperms, and seed coats, were analyzed based on the MtExpress database. The gene expression values are represented by trimmed mean of M (TMM) values⁵⁵. Genes with TMM values below 1.00 were considered to be non-expressed, while those with TMM values between 1.00 and 5.00 were classified as lowly expressed, those between 5.00 and 20.00 as moderately expressed, and those above 20.00 as highly expressed⁵⁶. As illustrated in Fig. 5 and Table S2, the *MtKCS* genes exhibited distinct expression profiles across the six *M. truncatula* organs. *MtKCS*3, 11, 12, 21, and 24 are not expressed in any of the analyzed tissues/organs, while the remaining 20 *MtKCS* genes are expressed in at least one of the analyzed tissues/organs. *MtKCS*2, 9, 13, 18, 19, and 23 were identified as being expressed in all examined organs and seed tissues. The high expression levels of *MtKCS*1, 2,

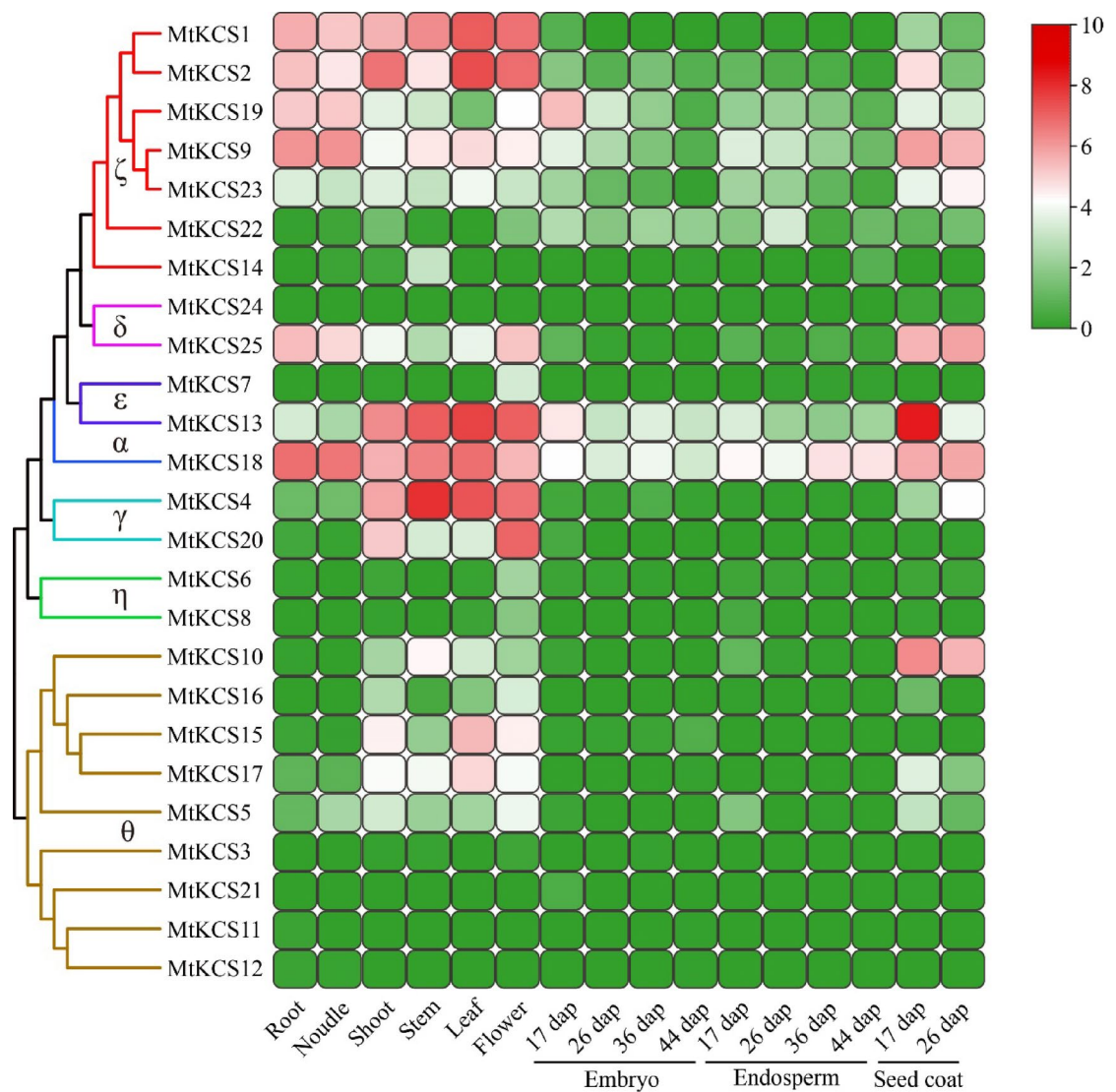


Fig. 5. Expression profiles of *MtKCS* genes in different organs and developing seed tissues. The color scale from green to red indicates the increased expression levels of the genes.

9, and 18 in all six organs indicate that these genes may play a pivotal role in the fundamental growth processes of *M. truncatula*. A number of genes exhibited high expression levels in specific tissues and organs. For instance, *MtKCS4*, 13, and 20 specifically expressed in above-ground organs, *MtKCS25* displayed high expression in roots, nodules, and flowers, while *MtKCS15* and *MtKCS17* exhibited high expression in shoots, leaves, and flowers. The expression of only six genes (*MtKCS9*, 13, 18, 19, 22, and 23) was observed in the developing embryo and endosperm. Among these genes, *MtKCS13* and *MtKCS18* were expressed in all stages, indicating a pivotal role in seed development. In developing seed coats, 11 *MtKCS* genes were identified as being expressed, with seven of them (*MtKCS2*, 9, 10, 13, 18, 23, and 25) exhibiting high expression levels.

Expression level of *MtKCS* genes in response to abiotic stress

To ascertain the putative functions of *MtKCS* genes in response to abiotic stresses, *M. truncatula* seedlings were treated with a range of stressors, including NaCl, PEG, 42 °C, and 4 °C, in order to simulate salt, drought, heat, and cold stress, respectively. Ten *MtKCS* genes that were expressed in leaves were selected for the purpose of determining their relative expression levels under abiotic stress using qRT-PCR (Fig. 6). In response to salt stress, *MtKCS9* and *MtKCS10* exhibited rapid and sustained downregulation, while the remaining genes displayed upregulation at the initial or intermediate time point. This suggests that these genes may play a crucial role in the early stages of the salt stress response. Following a 12-hour period of salt treatment, the expression levels of all *MtKCS* genes were found to be depressed. The expression of *MtKCS2*, 9, 10, 13, 15, 17, and 18 was induced by drought stress at 2 h, 4 h, or 6 h after treatment. *MtKCS9* and 10 exhibited a more than five-fold increase at certain time points, suggesting that they may play a role in the response to drought stress. In response to heat stress, *MtKCS2*, 10, 13, 15, 17, and 18 exhibited a notable increase in expression at 4, 6, or 12 h post-treatment, whereas the remaining genes displayed a consistent decline in expression at the majority of time

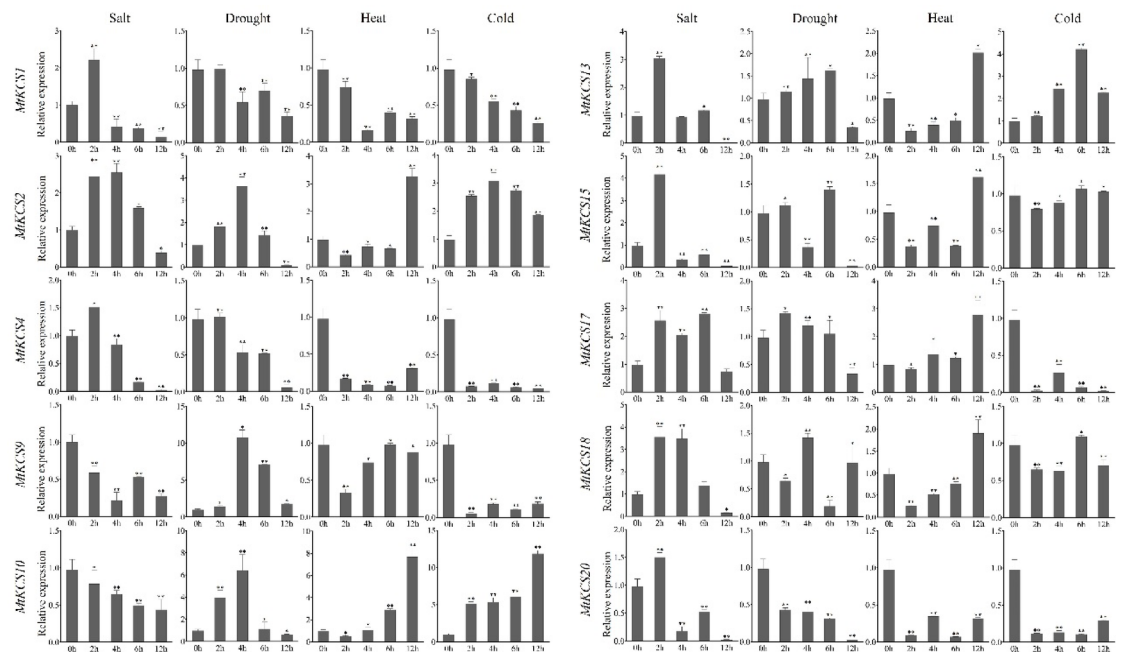


Fig. 6. Relative expression levels of *MtKCS* genes under heat, cold, salt, and drought stress in *M. truncatula*. qRT-PCR was used to examine the expression levels of ten leaf-expressed *MtKCS* genes in triplicate.

points. In response to cold stress, *MtKCS2*, *10*, and *13* exhibited a constant up-regulation, while the other genes demonstrated a significant down-regulation. Of particular interest is the observation that the expression level of *MtKCS10* was increased by more than five-fold under cold stress, indicating its potential as a crucial factor in cold stress tolerance.

Discussion

Epidermal cuticular waxes constitute a vital component of the plant cuticle, serving as the primary physical barrier to mitigate nonstomatal water loss and combat environmental stressors such as drought, salinity, UV radiation, pathogens, and insects^{3,7,8}. VLCFAs and their derivatives act as essential precursors for synthesizing sphingolipids, suberin, and cuticular wax¹⁰. KCSs catalyze the rate-limiting step in VLCFA biosynthesis, directly regulating plant growth, developmental processes, and stress resistance^{9,10}. The systematic identification and analysis of the KCS gene family will provide not only a physiological and molecular basis for understanding the biosynthesis of VLCFAs, but also facilitate the exploration of the molecular regulatory mechanisms that underpin plant responses to stress.

Genome-wide analyses of KCS genes have been reported in multiple angiosperms (typically contain >20 KCS members)^{33,35,36,57,58}, yet remain unexplored in *M. truncatula*, the well known legume model plant⁴⁸. Here, we identified 25 *MtKCS* genes in its genome, all exhibiting conserved ACP_syn_III_C and FAEL1_CUT1_RppA domains (Fig. 1A). This number is comparable to that observed in other diploid plants, such as *Arabidopsis* (21 members)²¹, rice (22 members)³³, sorghum (25 members)³⁵, and maize (26 members)³⁶. Gene duplication, which encompasses both tandem and segmental duplication, represents a fundamental source of new genes in the evolutionary process, contributing to the expansion of gene families and functional differentiation^{54,59}. Tandem and segmental duplication has been observed among KCS gene family in a number of species, including *Arabidopsis*, apple, sorghum, and barley^{21,35,58,60}. This study identified four segmentally and four tandemly duplicated gene pairs in the *MtKCS* family. All of the segmental duplicated gene pairs exhibited Ka/Ks ratios < 1 (Table S2), indicating purifying selection occurred during evolution. Collinearity analysis revealed 12 and 36 orthologous gene pairs between *M. truncatula* and *Arabidopsis*/soybean, respectively (Fig. 1B), with nine *MtKCS* genes showing collinearity to both species, supporting conserved evolution of plant KCS genes from a common ancestor⁵⁷. This result suggests that they may have been conserved during evolution and perform analogous functions in disparate plant species. Gene duplication events and syntenic relationships collectively shaped the functional diversity of the *MtKCS* family. The tandem-duplicated pair *MtKCS15* and *MtKCS17* retained structural conservation (Fig. 3) but diverged in shoot- versus leaf-predominant expression (Fig. 5), indicating that regulatory divergence (e.g., promoter *cis*-element variation) drives subfunctionalization to partition cuticular wax. In contrast, *MtKCS25* is an ortholog of *AtKCS1*, which directly regulates the biosynthesis of C26-C30 wax alcohols and aldehydes in *Arabidopsis*^{22,42}. While *AtKCS1* is predominantly expressed in leaves and stems, *MtKCS25* exhibits root-specific expression, suggesting functional divergence during evolution. Given its high expression in roots, we hypothesize that *MtKCS25* may contribute to root cuticular wax deposition, potentially enhancing barrier functions against soil-borne pathogens or abiotic stresses.

In general, genes that are clustered in the same evolutionary clade often demonstrate similar biological functions⁶¹. In the present study, 157 KCS proteins from *Arabidopsis*, turnip, *M. truncatula*, soybean, rice, and sorghum were categorized into nine groups (Fig. 2), which is in accordance with previous reports^{21,38,62}. Subsequent gene structure and motif analyses demonstrated that *MtKCS* genes within the same groups exhibited a high degree of conservation (Fig. 3), providing further support for the phylogenetic classification. It is noteworthy that genes in groups λ and η are exclusive to monocotyledonous and dicotyledonous plants, respectively (Fig. 2; Table 2). This indicates that these genes were formed during the period when dicots and monocots diverged, and it is possible that such genes have undergone functional differentiation. Furthermore, our findings revealed that *KCSs* in group β were exclusively present in two cruciferous plants, *Arabidopsis* and turnip, a discovery that has been previously documented in other studies^{38,41,63}. It is noteworthy that the number of *KCS* genes in each group differed significantly between species. With regard to dicotyledonous plants, the number of *AtKCS* genes ranged from two to three, while the number of *BrKCS* genes ranged from three to five or six. In the case of λ , the number of *BrKCS* genes was higher. In contrast, the number of *MtKCS* and *GmKCS* genes varied considerably. Groups ζ and θ comprise more than seven members, whereas the remaining groups have no more than four members (Fig. 2). The significant disparity in the number of members within each group suggests that both gene loss and duplication events have occurred during their evolutionary history. The functional differentiation of these genes represents a significant area of research. Among higher plants, the function of *AtKCS* genes has been the most thoroughly investigated, with dozens of *KCS* genes from other plants also having been functionally characterized^{24,26,29,64}. The homologous relationship between *MtKCS* and *KCS* genes from other plants offered certain insights into their functional exploration.

As a vestige of evolutionary history, the intron/exon configuration reflects the evolutionary trajectory of a gene family. An analysis of exon-intron structures may offer cues into the evolutionary history of specific gene families⁶⁵. Similar with previous reports^{21,38,58,60}, the *MtKCS* genes exhibit simple gene structures, with the majority (19 out of 25) lacking introns. Only members from groups ϵ and ζ had one or two introns, a phenomenon that is also present in soybean³⁸. Besides promoter, intron may also be an integral part of the regulatory program controlling gene expression level^{66,67}. Plants with fewer or shorter introns exhibit enhanced adaptive capacity, likely reflecting active evolutionary selection for regulatory efficiency^{68,69}. The connection between intron presence and *MtKCS* gene expression/functional specialization warrants deeper exploration. Promoter *cis*-element composition critically regulates gene functionality, emphasizing the need to characterize these regulatory features in evolutionary studies⁷⁰. The identification of the upstream *cis*-acting elements of *MtKCS* genes will facilitate a more comprehensive understanding of the mechanisms underlying their expression regulation. In accordance with prior findings regarding the *KCS* gene family^{35,58,71}, *cis*-acting elements associated with hormone and stress responses were observed to be extensively distributed in *MtKCS* promoters. All *MtKCS* promoters were found to contain at least one hormone and stress response element. Prior research has demonstrated that these elements are implicated in the control of gene expression in response to diverse stressors³⁹. These findings indicate that *MtKCS* expression regulation is highly intricate and may be involved in the control of growth and abiotic stress resistance in *M. truncatula* plants.

It has been reported that *KCS* genes display a distinctive expression profile across a range of tissues. For instance, *AtKCS6* was found to be highly expressed in flowers and siliques, but not in roots. *AtKCS17* was observed to be expressed exclusively in flowers and siliques, while *AtKCS18* and *AtKCS19* exhibited preferential expression in seeds^{21,72,73}. An investigation into the expression profiles of *MtKCS* genes may facilitate the elucidation of their potential roles in plant physiological processes and development. The expression patterns of each *MtKCS* gene in six organs and different tissues of developing seeds were obtained from public databases. Twenty of the 25 *MtKCS* genes exhibited expression in at least one tissue or organ, while the remaining five demonstrated no expression in any tissue or organ (Fig. 5; Table S3). In contrast, *MtKCS2*, 9, 13, 18, 19, 23, and 25 were found to be expressed throughout the plant. In the six examined organs, *MtKCS1*, 2, 9, and 18 exhibited a consistently high expression level. Additionally, certain members were expressed in specific tissues/organs. For instance, *MtKCS4/20* expression was restricted to aerial organs, whereas *MtKCS19/25* expressed in roots, nodules, and flowers, and *MtKCS15/17* were detected in shoots, leaves, and flowers (Fig. 5; Table S3). *AtKCS18*, the first *KCS* gene cloned in higher plants, is seed-specific and essential for VLCFA synthesis and lipid storage in *Arabidopsis*¹⁶. Notably, *MtKCS18*, the closest homolog of *AtKCS18*, showed exclusive high expression in *M. truncatula* developing endosperm, suggesting functional conservation. These tissue-specific expression patterns of *MtKCS* genes imply functional diversification and warrant further exploration.

Abiotic stressors frequently have a deleterious or even lethal impact on the growth and development of *M. truncatula*^{74,75}. An increasing body of evidence indicates that plant *KCS* genes play a role in the response to and adaptation to abiotic stress^{10,46,76}. The active expression response of the *KCS* gene *TaCer6* is positively correlated with the drought- and cold-tolerance abilities of different wheat (*Triticum aestivum*) cultivars⁷⁷. The overexpression of *BnKCS1-1*, *BnKCS1-1*, and *BnCER1-2* in rapeseed resulted in an increase in wax crystal density on the leaf surface and an enhancement in the drought tolerance of the transgenic plants⁴³. The ectopic expression of *CsKCS6* from orange, a gene that exhibits significantly altered expression under conditions of drought, salt stress, and abscisic acid treatment, has been demonstrated to enhance the abiotic stress tolerance of *Arabidopsis*⁴⁴. In *M. sativa*, the expression level of *MsKCS10* (which is homologous to *MtKCS13* in this study) was found to significantly increase under drought conditions. The overexpression of *MsKCS10* in tobacco and tomato plants has been demonstrated to enhance their drought tolerance ability, with this effect being attributed to the regulation of cuticular wax biosynthesis and morphology⁴⁶. Prior research has established that transcriptional regulation of *KCS* genes is essential for coordinating plant growth, development, and abiotic stress adaptation. For example, this regulatory conservation extends to defense responses—in *Arabidopsis*, *MYB30* activates the hypersensitive cell death response by modulating VLCFA biosynthesis⁷⁸. Similarly, in *Populus tomentosa*, the MYB transcription factor *PtoMYB142* enhances drought tolerance by directly binding to promoters of wax

biosynthesis genes (*CER4*, *KCS6*) and upregulating their expression under drought stress⁷⁹. Furthermore, light-responsive *cis*-elements such as the G-box coordinate developmental processes; in sorghum, G-box-mediated regulation of *KCS* genes influences flowering time³⁵. In the present study, we examined the transcriptional profiles of ten leaf-expressed *MtKCS* gene family members under conditions of drought, salt, heat, and cold stress. All genes examined exhibited significant changes following abiotic stress treatment, although their response patterns diverged among different stresses (Fig. 6). For instance, *MtKCS9* exhibited consistent down-regulation under salt and cold stress conditions, whereas its expression level was markedly elevated following drought treatment. Furthermore, *MtKCS10* demonstrated increased expression at the majority of time points following drought, heat, and cold treatments, whereas its expression was significantly suppressed by salt stress. These findings suggest that different *MtKCS* genes may have distinct roles in the abiotic stress response of *M. truncatula* plants. The results of our experiment provide a list of candidate stress-response related *MtKCS* genes that will be valuable for further functional research. As reported by previous studies, circadian rhythms influence the expression of a large number of genes in plants⁸⁰. Furthermore, rhythmic expression of abiotic stress-responsive genes under constant conditions has also reported in many plant species^{81–83}. The fluctuating expression level changes of abiotic stress-responsive genes during the developmental process of *M. truncatula* seedlings were also reported by many studies^{84,85}. Due to the lack of a mock control for each time point during the time course of abiotic stress treatment in our study, the influence of developmental process or circadian rhythms on *MtKCS* gene expression cannot be ruled out. A more comprehensive experimental design is needed in the future to determine the key factors that affect the expression level of *MtKCS* genes.

Materials and methods

Identification of *MtKCS* genes

The datasets of the *M. truncatula* genome (accession Jemalong A17) were obtained from the *Medicago* website (<https://medicago.toulouse.inra.fr/MtrunA17r5.0-ANR/>)⁸⁶. The Hidden Markov Model profiles of the two conserved domains (PF08392 for FAE1_CUT1_RppA, and PF08541 for ACP_syn_III_C) of *KCS* proteins were obtained from the InterPro website (<https://www.ebi.ac.uk/interpro/>). The HMMER software (<http://www.hmm.org/>) was utilized to search the sequences with these domains from the *M. truncatula* genome, with an *E*-value threshold of 10^{-5} . Additionally, protein sequences of 21 AtKCS were obtained from the *Arabidopsis* Information Resource (TAIR) database (<https://www.arabidopsis.org/>) and subjected to BLASTP (<https://blast.ncbi.nlm.nih.gov/Blast.cgi>) comparisons against the *M. truncatula* protein database (*E*-value $< 10^{-5}$). Subsequently, the non-redundant protein sequences were submitted to the NCBI conserved domains website (<https://www.ncbi.nlm.nih.gov/Structure/cdd/wrpsb.cgi>) and the InterPro website to ascertain the presence of the two conserved domains. Proteins that exhibited both of ACP_syn_III_C and the FAE1_CUT1_RppA domains were identified as members of the *KCS* gene family in *M. truncatula*.

Prediction of the physicochemical properties, subcellular localization, and TAH of *MtKCS* proteins

The ProtParam tool (<https://web.expasy.org/protparam/>) was utilized to predict the physicochemical properties of *MtKCS* proteins, including molecular weight, theoretical isoelectric point, instability index, aliphatic index, and the grand average of hydropathy index (GRAVY). The subcellular location and the transmembrane alpha-helix (TAH) of *MtKCS* proteins were predicted using the WoLF PSORT web server (<https://wolfsort.hgc.jp/>) and the TMHMM website (<https://services.healthtech.dtu.dk/service.php?TMHMM-2.0>), respectively.

Chromosomal localization and synteny analysis of *MtKCS* genes

The chromosomal locations of *MtKCS* genes were obtained from the GFF3 file, which is part of the *M. truncatula* genome datasets. The *MtKCS* genes were mapped onto the *M. truncatula* chromosomes based on their physical locations. A Multiple Collinear Scanning Toolkit (MCScanX) was utilized to examine collinear blocks of *KCS* genes across *M. truncatula*, *Arabidopsis*, and soybean, with the results visualized by TBtools. To assess the evolutionary divergence between duplicated *KCS* genes, the non-synonymous substitution rate (*Ka*) and synonymous substitution rate (*Ks*) of each gene pair were calculated using the *Ka/Ks*_Calculator plugin in TBtools software⁴².

Phylogenetic analysis of *KCS* proteins

The alignment of *KCS* protein sequences from *Arabidopsis*²¹, turnip⁴¹, rice³³, sorghum³⁵, soybean³⁸ and *M. truncatula* was conducted using the ClustalX software (<http://www.clustal.org/>). A phylogenetic tree was constructed using the neighbor-joining method with MEGA 11.0 software (<https://www.megasoftware.net/>), with parameters including pairwise deletions, a Poisson model, and 1,000 bootstrap replications⁸⁷.

Analysis of gene structure and conserved motifs of *MtKCS* genes

The GFF3 file of *M. truncatula* was utilized for the analysis of the examination of the exon/intron structure of *MtKCS* genes. The Multiple Expectation Maximization for Motif Elicitation (MEME) tool (<http://meme-suite.org/>) was employed to investigate the conserved motifs of the *MtKCS* proteins, with a maximum of 10 motifs and an optimum motif width of 6–50 amino acid residues.

Prediction of *cis*-acting elements in *MtKCS* promoters

The 2.0 kb upstream sequences of the *MtKCS* open reading frames were extracted from the *M. truncatula* genome sequence and considered as the promoter region. The PlantCARE website (<https://bioinformatics.psb.u Gent.be/webtools/plantcare/html/>) was employed to predict *cis*-acting elements, and Excel software (<https://www.microsoft.com/>) was used to display the number and type of each *cis*-acting element.

Expression pattern of *MtKCS* genes in various tissues/organs

The RNA-seq data from the root, nodule, shoot, stem, leaf, flower, and developing embryo, endosperm, and seed coat of *M. truncatula* were obtained from the MtExpress database (<https://lipm-browsers.toulouse.inra.fr/pub/expressAtlas>). The expression levels of each gene were represented by the TMM values⁵⁵, and a heatmap illustrating the tissue-specific expression profiles was generated using the log₂-transformed (TMM + 1) values of *MtKCS* genes in the TBtools software.

Plant growth and stress treatments of *M. truncatula* seedlings

The *M. truncatula* (accession Jemalong A17) seeds used in this study were stored at the College of Agriculture and Biology, Liaocheng University. The *M. truncatula* seeds were kindly provided by Professor Xin Chen in College of life science, Zhejiang University. The seeds were soaked in 98% concentrated sulfuric acid for a period of ten minutes in order to break the seed coat. They were then rinsed five times with ultrapure water, and placed in Petri dishes at a temperature of 25 °C to facilitate germination. Once the root had reached a length of approximately 2 cm, uniform *M. truncatula* seedlings were selected and transplanted into square pots with a 1:1 ratio of vermiculite to nutrient soil. The seedlings were cultivated in a growth chamber with a 16-hour light period and an 8-hour dark period, and a temperature cycle of 25 °C during the day and 20 °C at night.

Following a four-week period, the seedlings were subjected to abiotic stress treatment. Prior to subjecting all seedlings to stress treatments, the roots were washed with water and placed in a Hoagland nutrient solution for hydroponics for a period of one day. For the purposes of inducing cold and heat stress, the seedlings were transferred to chambers with temperatures set at 4 °C and 42 °C, respectively^{88,89}. For the purposes of this study, salt and drought stress were applied to the seedlings via hydroponics, with the Hoagland solution containing 300 mM NaCl or 15% PEG6000 (w/v), respectively^{74,90}. Leaves were collected at 0, 2, 4, 6, and 12 h post-treatment. The samples were immediately frozen in liquid nitrogen and subsequently stored at -80 °C until RNA extraction. Each sample was derived from five individual plants, and three biological replicates were utilized in each experiment.

RNA extraction, cDNA synthesis, and qRT-PCR analysis

Total RNA was extracted using the TSINGKE RNA extraction kit (TSP401). Samples were pulverized in liquid nitrogen, and 100 mg of powder was mixed with 600 µL Buffer PSL for gDNA removal. RNA was purified using 700 µL RWA and 500 µL RWB, then eluted in 40 µL RNase-free ddH₂O. cDNA was synthesized with the Prime Script RT kit (TSINGKE, TSK301S) and stored at -20 °C. qRT-PCR was performed using the SYBR Green kit (TSINGKE, TSE201) on a LightCycler[®] 480 instrument with the following program: 95 °C for 30 s; 40 cycles of 95 °C for 5 s and 60 °C for 30 s; and a melting curve. The 2^{-ΔΔCt} method was used for relative quantification⁹¹, with *MtActin* (*Medtr3g095530*)⁹² as the internal control. Data were analyzed using GraphPad Prism 8.0 (<http://www.graphpad.com/>), presented as mean ± SE of three replicates, and assessed for significance (**P* < 0.05, ***P* < 0.01) via *t*-test. Primers are listed in Table S1.

Data availability

All data generated or analysed during this study are included in this published article and its supplementary information files.

Received: 1 January 2025; Accepted: 30 April 2025

Published online: 07 May 2025

References

1. Peck, S. & Mittler, R. Plant signaling in biotic and abiotic stress. *J. Exp. Bot.* **71**, 1649–1651. <https://doi.org/10.1093/jxb/eraa051> (2020).
2. Zandalinas, S. I. & Mittler, R. Plant responses to multifactorial stress combination. *New. Phytol.* **234**, 1161–1167. <https://doi.org/10.1111/nph.18087> (2022).
3. Lewandowska, M., Keyl, A. & Feussner, I. Wax biosynthesis in response to danger: its regulation upon abiotic and biotic stress. *New. Phytol.* **227**, 698–713. <https://doi.org/10.1111/nph.16571> (2020).
4. Xu, L. et al. A genome-wide association study identifies genes associated with cuticular wax metabolism in maize. *Plant. Physiol.* **194**, 2616–2630. <https://doi.org/10.1093/plphys/kiae007> (2024).
5. Xue, D. et al. Molecular and evolutionary mechanisms of cuticular wax for plant drought tolerance. *Front. Plant. Sci.* **621** <https://doi.org/10.3389/fpls.2017.00621> (2017).
6. Zhu, J. et al. Characterization of cuticular wax in tea plant and its modification in response to low temperature. *J. Agric. Food Chem.* **70**, 13849–13861. <https://doi.org/10.1021/acs.jafc.2c05470> (2022).
7. Yeats, T. H. & Rose, J. K. The formation and function of plant cuticles. *Plant. Physiol.* **163**, 5–20. <https://doi.org/10.1104/pp.113.22> (2013).
8. Lee, S. B. & Suh, M. C. Regulatory mechanisms underlying cuticular wax biosynthesis. *J. Exp. Bot.* **73**, 2799–2816. <https://doi.org/10.1093/jxb/erab509> (2022).
9. Haslam, T. M. & Kunst, L. Extending the story of very-long-chain fatty acid elongation. *Plant. Sci.* **210**, 93–107. <https://doi.org/10.1016/j.plantsci.2013.05.008> (2013).
10. Batsale, M. et al. Biosynthesis and functions of very-long-chain fatty acids in the responses of plants to abiotic and biotic stresses. *Cells* **10**, 1284. <https://doi.org/10.3390/cells10061284> (2021).
11. Chai, G. et al. Three Endoplasmic reticulum-associated fatty acyl-coenzyme reductases were involved in the production of primary alcohols in hexaploid wheat (*Triticum aestivum* L.). *BMC Plant. Biol.* **18**, 41. <https://doi.org/10.1186/s12870-018-1256-y> (2018).
12. Zhao, L., Haslam, T. M., Sonntag, A., Molina, I. & Kunst, L. Functional overlap of long-chain acyl-CoA synthetases in *Arabidopsis*. *Plant. Cell. Physiol.* **60**, 1041–1054. <https://doi.org/10.1093/pcp/pcz019> (2019).
13. Kim, J., Kim, R. J., Lee, S. B. & Suh, M. C. Protein-protein interactions in fatty acid elongase complexes are important for very-long-chain fatty acid synthesis. *J. Exp. Bot.* **73**, 3004–3017. <https://doi.org/10.1093/jxb/erab543> (2022).
14. Millar, A. A. & Kunst, L. Very-long-chain fatty acid biosynthesis is controlled through the expression and specificity of the condensing enzyme. *Plant. J.* **12**, 121–131. <https://doi.org/10.1046/j.1365-3113.1997.12010121.x> (1997).

15. Fan, Y., Yuan, C., Jin, Y., Hu, G. R. & Li, F. L. Characterization of 3-ketoacyl-CoA synthase in a nervonic acid producing oleaginous microalgae *Mychonastes* afer. *Algal Res.* **31**, 225–231. <https://doi.org/10.1016/j.algal.2018.02.017> (2018).
16. James, D. et al. Directed tagging of the *Arabidopsis* FATTY ACID ELONGATION1 (*FAE1*) gene with the maize transposon activator. *Plant. Cell.* **7**, 309–319. <https://doi.org/10.1105/tpc.7.3.309> (1995).
17. Katavic, V. et al. Restoring enzyme activity in nonfunctional low erucic acid brassica napus fatty acid elongase 1 by a single amino acid substitution. *Eur. J. Biochem.* **269**, 5625–5631. <https://doi.org/10.1046/j.1432-1033.2002.03270.x> (2002).
18. Rossak, M., Smith, M. & Kunst, L. Expression of the *FAE1* gene and *FAE1* promoter activity in developing seeds of *Arabidopsis thaliana*. *Plant. Mol. Biol.* **46**, 717–725. <https://doi.org/10.1023/a:1011603923889> (2001).
19. Sagar, M., Pandey, N., Qamar, N., Singh, B. & Shukla, A. Domain analysis of 3 Keto acyl-CoA synthase for structural variations in *Vitis vinifera* and *Oryza brachyantha* using comparative modelling. *Interdiscip. Sci.* **7**, 7–20. <https://doi.org/10.1007/s12539-013-0017-8> (2015).
20. Funai, N., Ohnishi, Y., Ebizuka, Y. & Horinouchi, S. Alteration of reaction and substrate specificity of a bacterial type III polyketide synthase by site-directed mutagenesis. *Biochem. J.* **367**, 781–789. <https://doi.org/10.1042/BJ20020953> (2002).
21. Joubès, J. et al. The VLCFA elongase gene family in *Arabidopsis thaliana*: phylogenetic analysis, 3D modelling and expression profiling. *Plant. Mol. Biol.* **67**, 547–566. <https://doi.org/10.1007/s11103-008-9339-z> (2008).
22. Todd, J., Post-Beittenmiller, D. & Jaworski, J. G. *KCS1* encodes a fatty acid elongase 3-ketoacyl-CoA synthase affecting wax biosynthesis in *Arabidopsis thaliana*. *Plant. J.* **17**, 119–130. <https://doi.org/10.1046/j.1365-3113.1999.00352.x> (1999).
23. Fiebig, A. et al. Alterations in *CER6*, a gene identical to *CUT1*, differentially affect long-chain lipid content on the surface of pollen and stems. *Plant. Cell.* **12**, 2001–2008. <https://doi.org/10.1105/tpc.12.12.2001> (2000).
24. Hooker, T. S., Millar, A. A. & Kunst, L. Significance of the expression of the *CER6* condensing enzyme for cuticular wax production in *Arabidopsis*. *Plant. Physiol.* **129**, 1568–1580. <https://doi.org/10.1104/pp.003707> (2002).
25. Kim, J., Lee, S. B. & Suh, M. C. *Arabidopsis* 3-ketoacyl-CoA synthase 4 is essential for root and pollen tube growth. *J. Plant. Biol.* **64**, 155–165. <https://doi.org/10.1007/s12374-020-09288-w> (2021).
26. Huang, H. et al. An ancestral role for 3-ketoacyl-CoA synthase 3 as a negative regulator of plant cuticular wax synthesis. *Plant. Cell.* **35**, 2251–2270. <https://doi.org/10.1093/plcell/koab051> (2023).
27. Franke, R. et al. The *DAISY* gene from *Arabidopsis* encodes a fatty acid elongase condensing enzyme involved in the biosynthesis of aliphatic Suberin in roots and the chalaza-micropyle region of seeds. *Plant. J.* **57**, 80–95. <https://doi.org/10.1111/j.1365-3113.2008.03674.x> (2009).
28. Lee, S. B. et al. Two *Arabidopsis* 3-ketoacyl coA synthase genes, *KCS20* and *KCS2/DAISY*, are functionally redundant in cuticular wax and root Suberin biosynthesis, but differentially controlled by osmotic stress. *Plant. J.* **60**, 462–475. <https://doi.org/10.1111/j.1365-3113.2009.03973.x> (2009).
29. Kim, J. et al. *Arabidopsis* 3-ketoacyl-coenzyme a synthase 9 is involved in the synthesis of tetracosanoic acids as precursors of cuticular waxes, suberins, sphingolipids, and phospholipids. *Plant. Physiol.* **162**, 567–580. <https://doi.org/10.1104/pp.112.2.10450> (2013).
30. Gray, J. E. et al. The HIC signalling pathway links CO₂ perception to stomatal development. *Nature* **408**, 713–716. <https://doi.org/10.1038/35047071> (2000).
31. Pruitt, R. E., Vielle-Calzada, J. P., Ploense, S. E., Grossniklaus, U. & Lolle, S. J. *FIDDLEHEAD*, a gene required to suppress epidermal cell interactions in *Arabidopsis*, encodes a putative lipid biosynthetic enzyme. *PNAS* **97**, 1311–1316. <https://doi.org/10.1073/pnas.97.3.1311> (2000).
32. Luzarowska, U. et al. Hello darkness, my old friend: 3-ketoacyl-coenzyme a synthase 4 is a branch point in the regulation of triacylglycerol synthesis in *Arabidopsis thaliana*. *Plant. Cell.* **35**, 1984–2005. <https://doi.org/10.1093/plcell/koab059> (2023).
33. Yang, L. et al. Genome-wide identification and expression analysis of 3-ketoacyl-CoA synthase gene family in rice (*Oryza sativa* L.) under cadmium stress. *Front. Plant. Sci.* **14**, 1222288. <https://doi.org/10.3389/fpls.2023.1222288> (2023).
34. Zheng, H. et al. Genome-scale analysis of the grapevine KCS genes reveals its potential role in male sterility. *Int. J. Mol. Sci.* **24**, 6510. <https://doi.org/10.3390/ijms24076510> (2023).
35. Zhang, A. et al. Genome-wide identification and characterization of the KCS gene family in sorghum (*Sorghum bicolor* (L.) Moench). *Peer J.* **10**, e14156. <https://doi.org/10.7717/peerj.14156> (2022).
36. Campbell, A. A. et al. A single-cell platform for reconstituting and characterizing fatty acid elongase component enzymes. *PloS One.* **14**, e0213620. <https://doi.org/10.1371/journal.pone.0213620> (2019).
37. Lian, X. Y. et al. *MdKCS2* increased plant drought resistance by regulating wax biosynthesis. *Plant Cell Rep.* **40**, 2357–2368. <https://doi.org/10.1007/s00299-021-02776-4> (2021).
38. Gong, Y. et al. Genome-wide identification and expression analysis of the KCS gene family in soybean (*Glycine max*) reveal their potential roles in response to abiotic stress. *Front. Plant. Sci.* **14**, 1291731. <https://doi.org/10.3389/fpls.2023.1291731> (2023).
39. Zhang, Y. et al. Wheat ABA receptor *TaPYL5* constitutes a signaling module with its downstream partners *TaPP2C53/TaSnRK2.1/TaABI1* to modulate plant drought response. *Int. J. Mol. Sci.* **24**, 7969. <https://doi.org/10.3390/ijms24097969> (2023).
40. Xiao, G. H., Wang, K., Huang, G. & Zhu, Y. X. Genome-scale analysis of the cotton KCS gene family revealed a binary mode of action for Gibberellin a regulated fiber growth. *J. Integr. Plant. Biol.* **58**, 577–589. <https://doi.org/10.1111/jipb.12429> (2016).
41. Xue, Y. et al. Genome-wide mining and comparative analysis of fatty acid elongase gene family in *Brassica napus* and its progenitors. *Gene* **747**, 144674. <https://doi.org/10.1016/j.gene.2020.144674> (2020).
42. Chen, L. et al. *AKR2A* interacts with *KCS1* to improve VLCFAs contents and chilling tolerance of *Arabidopsis thaliana*. *Plant. J.* **103**, 1575–1589. <https://doi.org/10.1111/tj.14848> (2020).
43. Wang, Q. et al. The β -ketoacyl-CoA synthase *KCS13* regulates the cold response in cotton by modulating lipid and Oxylin biosynthesis. *J. Exp. Bot.* **71**, 5615–5630. <https://doi.org/10.1093/jxb/eraa254> (2020).
44. Guo, W. et al. Ectopic expression of *CsKCS6* from navel orange promotes the production of very-long-chain fatty acids (VLCFAs) and increases the abiotic stress tolerance of *Arabidopsis thaliana*. *Front. Plant. Sci.* **11**, 564656. <https://doi.org/10.3389/fpls.2020.564656> (2020).
45. Yang, Z. et al. Overexpression of β -ketoacyl-CoA synthase from *Vitis vinifera* L. improves salt tolerance in *Arabidopsis thaliana*. *Front. Plant. Sci.* **11**, 564385. <https://doi.org/10.3389/fpls.2020.564385> (2020).
46. Wang, Y. et al. A 3-ketoacyl-CoA synthase 10 (*KCS10*) homologue from alfalfa enhances drought tolerance by regulating cuticular wax biosynthesis. *J. Agric. Food Chem.* **71**, 14493–14504. <https://doi.org/10.1021/acs.jafc.3c03881> (2023).
47. Lewis, G., Schrire, B., Mackinder, B. & Lock, M. Legumes of the world: Royal botanical gardens, kew. (2005).
48. Young, N. D. & Udvardi, M. Translating *Medicago truncatula* genomics to crop legumes. *Curr. Opin. Plant. Biol.* **12**, 193–201. <https://doi.org/10.1016/j.pbi.2008.11.005> (2009).
49. Yang, T. et al. The 3-ketoacyl-CoA synthase *WFL* is involved in lateral organ development and cuticular wax synthesis in *Medicago truncatula*. *Plant. Mol. Biol.* **105**, 193–204. <https://doi.org/10.1007/s11103-020-01080-1> (2021).
50. Chai, M. et al. A seed coat-specific β -ketoacyl-CoA synthase, *KCS12*, is critical for preserving seed physical dormancy. *Plant. Physiol.* **186**, 1606–1615. <https://doi.org/10.1093/plphys/kiab152> (2021).
51. Ghanevati, M. & Jaworski, J. G. Engineering and mechanistic studies of the *Arabidopsis* *FAE1* beta-ketoacyl-CoA synthase, *FAE1* KCS. *Eur. J. Biochem.* **269**, 3531–3539. <https://doi.org/10.1046/j.1432-1033.2002.03039.x> (2002).
52. Xu, G., Guo, C., Shan, H. & Kong, H. Divergence of duplicate genes in exon-intron structure. *PNAS* **109**, 1187–1192. <https://doi.org/10.1073/pnas.1109047109> (2012).

53. Zhou, T. et al. Genome-wide identification of NBS genes in Japonica rice reveals significant expansion of divergent *non-TIR* NBS-LRR genes. *Mol. Genet. Genomics*. **271**, 402–415. <https://doi.org/10.1007/s00438-004-0990-z> (2004).
54. Panchy, N., Lehti-Shiu, M. & Shiu, S. H. Evolution of gene duplication in plants. *Plant. Physiol.* **171**, 2294–2316. <https://doi.org/10.1104/pp.16.00523> (2016).
55. Carrere, S., Verdier, J. & Gamas, P. MtExpress, a comprehensive and curated RNAseq-based gene expression atlas for the model legume *Medicago truncatula*. *Plant. Cell. Physiol.* **62**, 1494–1500. <https://doi.org/10.1093/pcp/pcab110> (2021).
56. Girard, I. J. et al. RNA sequencing of *Brassica napus* reveals cellular redox control of sclerotinia infection. *J. Exp. Bot.* **68**, 5079–5091. <https://doi.org/10.1093/jxb/erx338> (2017).
57. Guo, H. S. et al. Evolution of the KCS gene family in plants: the history of gene duplication, sub/neofunctionalization and redundancy. *MGG* **291**, 739–752. <https://doi.org/10.1007/s00438-015-1142-3> (2016).
58. Lian, X. Y. et al. Genome wide analysis and functional identification of *MdKCS* genes in Apple. *Plant. Physiol. Biochem.* **151**, 299–312. <https://doi.org/10.1016/j.plaphy.2020.03.034> (2020).
59. Cannon, S. B., Mitra, A., Baumgarten, A., Young, N. D. & May, G. The roles of segmental and tandem gene duplication in the evolution of large gene families in *Arabidopsis thaliana*. *BMC Plant. Biol.* **4**, 10. <https://doi.org/10.1186/1471-2229-4-10> (2004).
60. Tong, T. et al. Genome-wide identification and expression pattern analysis of the KCS gene family in barley. *Plant. Growth Regul.* **93**, 89–103 (2021).
61. Liu, C., Wright, B., Allen-Vercos, E., Gu, H. & Beiko, R. Phylogenetic clustering of genes reveals shared evolutionary trajectories and putative gene functions. *Genome Biol. Evol.* **10**, 2255–2265. <https://doi.org/10.1093/gbe/evy178> (2018).
62. Rui, C. et al. Identification and structure analysis of KCS family genes suggest their responding to regulate fiber development in long-staple cotton under salt-alkaline stress. *Front. Genet.* **13**, 812449. <https://doi.org/10.3389/fgene.2022.812449> (2022).
63. Khan, U. M. et al. Comparative phylogenomic insights of KCS and ELO gene families in Brassica species indicate their role in seed development and stress responsiveness. *Sci. Rep.* **13**, 3577. <https://doi.org/10.1038/s41598-023-28665-2> (2023).
64. Huang, Z. et al. Heterologous expression of *MfWRKY7* of resurrection plant *myrothamnus flabellifolia* enhances salt and drought tolerance in *Arabidopsis*. *Int. J. Mol. Sci.* **23** <https://doi.org/10.3390/ijms23147890> (2022).
65. Wang, B., Xu, W., Tan, M., Xiao, Y. & Yang, H. Integrative genomic analyses of a novel cytokine, interleukin-34 and its potential role in cancer prediction. *Int. J. Mol. Sci.* **35**, 92–102. <https://doi.org/10.3892/ijmm.2014.2001> (2015).
66. Rose, A. B., Carter, A., Korf, I. & Kojima, N. Intron sequences that stimulate gene expression in *Arabidopsis*. *Plant. Mol. Biol.* **92**, 337–346. <https://doi.org/10.1007/s11103-016-0516-1> (2016).
67. Shaul, O. How introns enhance gene expression. *Int. J. Biochem. Cell. Biol.* **91**, 145–155. <https://doi.org/10.1016/j.biocel.2017.06.016> (2017).
68. Jin, Z., Xu, W. & Liu, A. Genomic surveys and expression analysis of *bZIP* gene family in castor bean (*Ricinus communis* L.). *Planta* **239**, 299–312. <https://doi.org/10.1007/s00425-013-1979-9> (2014).
69. Mattick, J. S. & Gagen, M. J. The evolution of controlled multitasked gene networks: the role of introns and other noncoding RNAs in the development of complex organisms. *Mol. Biol. Evol.* **18**, 1611–1630. <https://doi.org/10.1093/oxfordjournals.molbev.a003951> (2001).
70. Sun, Z. et al. Molecular traits and functional exploration of *BES1* gene family in plants. *Int. J. Mol. Sci.* **23**, 4242. <https://doi.org/10.3390/ijms23084242> (2022).
71. Rizwan, H. et al. Genome-wide identification and expression profiling of KCS gene family in passion fruit (*Passiflora edulis*) under fusarium Kyushuense and drought stress conditions. *Front. Plant. Sci.* **13**, 872263. <https://doi.org/10.3389/fpls.2022.872263> (2022).
72. Costaglioli, P. et al. Profiling candidate genes involved in wax biosynthesis in *Arabidopsis thaliana* by microarray analysis. *Acta Biochim. Biophys. Sin.* **1734**, 247–258. <https://doi.org/10.1016/j.bbali.2005.04.002> (2005).
73. Suh, M. C. et al. Cuticular lipid composition, surface structure, and gene expression in *Arabidopsis* stem epidermis. *Plant. Physiol.* **139**, 1649–1665. <https://doi.org/10.1104/pp.105.070805> (2005).
74. Song, J. et al. The U-box family genes in *Medicago truncatula*: key elements in response to salt, cold, and drought stresses. *PLoS One*. **12**, e0182402. <https://doi.org/10.1371/journal.pone.0182402> (2017).
75. Chen, Z., Ly Vu, B., Leprince, O. & Verdier, J. RNA sequencing data for heat stress response in isolated *medicago truncatula* seed tissues. *Data Brief*. **35**, 106726. <https://doi.org/10.1016/j.dib.2021.106726> (2021).
76. Kotoka, D. K. & Weiguo, Z. Molecular cloning and expression of 3-ketoacyl-CoA synthase (*3Kcs*) gene in mulberry (*Morus Alba* L.) under abiotic stresses. *Res. J. Biotechnol.* **13**, 1–7. <https://doi.org/10.23880/oajar-16000239> (2018).
77. Hu, X. J., Zhang, Z. B., Fu, Z. Y., Xu, P. & Hu, S. B. Significance of a β -ketoacyl-CoA synthase gene expression for wheat tolerance to adverse environments. *Plant. Biol.* **54**, 575–578. <https://doi.org/10.1007/s10535-010-0103-2> (2010).
78. Raffaele, S. et al. A MYB transcription factor regulates very-long-chain fatty acid biosynthesis for activation of the hypersensitive cell death response in *Arabidopsis*. *Plant. Cell.* **20**, 752–767. <https://doi.org/10.1105/tpc.107.054858> (2008).
79. Song, Q. et al. *PtoMYB142*, a Poplar *R2R3-MYB* transcription factor, contributes to drought tolerance by regulating wax biosynthesis. *Tree Physiol.* **42**, 2133–2147. <https://doi.org/10.1093/treephys/tpac060> (2022).
80. Creux, N. & Harmer, S. Circadian rhythms in plants. *Cold Spring Harbor Perspect. Biol.* **11**, a034611. <https://doi.org/10.1101/cshperspect.a034611> (2019).
81. Habte, E., Müller, L. M., Shtaya, M., Davis, S. J. & von Korff, M. Osmotic stress at the barley root affects expression of circadian clock genes in the shoot. *Plant. Cell. Environ.* **37**, 1321–1327. <https://doi.org/10.1111/pce.12242> (2014).
82. Marcolino-Gomes, J. et al. Diurnal oscillations of soybean circadian clock and drought responsive genes. *PLoS One*. **9**, e86402. <https://doi.org/10.1371/journal.pone.0086402> (2014).
83. Grundy, J., Stoker, C. & Carré, I. A. Circadian regulation of abiotic stress tolerance in plants. *Front. Plant. Sci.* **6**, 648. <https://doi.org/10.3389/fpls.2015.00648> (2015).
84. Liu, R., Guo, Z. & Lu, S. Genome-Wide identification and expression analysis of the Aux/IAA and auxin response factor gene family in *Medicago truncatula*. *Int. J. Mol. Sci.* **22**, 10494. <https://doi.org/10.3390/ijms221910494> (2021).
85. Yu, S. et al. Genome-Wide identification and characterization of Short-Chain dehydrogenase/reductase (SDR) gene family in *Medicago truncatula*. *Int. J. Mol. Sci.* **22**, 9498. <https://doi.org/10.3390/ijms22179498> (2021).
86. Pecrix, Y. et al. Whole-genome landscape of *Medicago truncatula* symbiotic genes. *Nat. Plants*. **4**, 1017–1025. <https://doi.org/10.1038/s41477-018-0286-7> (2018).
87. Kumar, S., Stecher, G. & Tamura, K. MEGA7: molecular evolutionary genetics analysis version 7.0 for bigger datasets. *Mol. Biol. Evol.* **33**, 1870–1874. <https://doi.org/10.1093/molbev/msw054> (2016).
88. Irshad, A., Rehman, R. N. U., Dubey, S., Khan, M. A. & Yang, P. Rhizobium inoculation and exogenous melatonin synergistically increased thermotolerance by improving antioxidant defense, photosynthetic efficiency, and nitro-oxidative homeostasis in *Medicago truncatula*. *Front. Ecol. Evol.* **10**, 945695. <https://doi.org/10.3389/fevo.2022.945695> (2022).
89. Li, Y. W., Lian, R. L. & Wang, X. M. Isolation and functional analysis of the low-temperature-responsive gene *MtHLH1* in *Medicago truncatula*. *Chin. Agric. Sci.* **45**, 3430–3436. <https://doi.org/10.5555/20123307274> (2012).
90. He, C., Du, W., Ma, Z., Jiang, W. & Pang, Y. Identification and analysis of flavonoid pathway genes in responsive to drought and salinity stress in *Medicago truncatula*. *J. Plant. Physiol.* **302**, 154320 (2024). <https://pubmed.ncbi.nlm.nih.gov/39111193/>
91. Derveaux, S., Vandesompele, J. & Hellemans, J. How to do successful gene expression analysis using real-time PCR. *Methods (San Diego Calif)*. **50**, 227–230. <https://doi.org/10.1016/j.ymeth.2009.11.001> (2010).
92. Hu, B. et al. *SWEET* gene family in *Medicago truncatula*: Genome-wide identification, expression and substrate specificity analysis. *Plants (Basel Switzerland)*. **8**, 338. <https://doi.org/10.3390/plants8090338> (2019).

Author contributions

Y.S. and P.C. were responsible for the conceptualisation of the study and the design of the experiments. P.L. and J.L. were responsible for bioinformatic analysis, stress treatment, material sampling, and gene expression experiments. Y.Z., X.Z., Q.S., W.Z., and Y.G. assisted with plant cultivation and RNA extraction. N.W. was involved in revising the manuscript. J.Y. and H.Z. contributing to data collection and analysis. Y.S., P.L., and J.L. wrote the manuscript. All authors read and approved the submitted version of the manuscript.

Funding

This work was financially supported by the Higher Educational Program of China for Cultivation of Young Innovative Talents (202410447005; CXCX2024310), the Key Funding Project for Cooperation Between Dongying City and Liaocheng University (SXHZ-2024-02-9), the Science and Technology Collaborative Innovation Project of Liaocheng City (2024XT10), and the Research on Key Engineering Technologies for Smart Agriculture of Liaocheng University (K23LD90).

Declarations

Competing interests

The authors declare no competing interests.

Additional information

Supplementary Information The online version contains supplementary material available at <https://doi.org/10.1038/s41598-025-00809-6>.

Correspondence and requests for materials should be addressed to P.C. or Y.S.

Reprints and permissions information is available at www.nature.com/reprints.

Publisher's note Springer Nature remains neutral with regard to jurisdictional claims in published maps and institutional affiliations.

Open Access This article is licensed under a Creative Commons Attribution-NonCommercial-NoDerivatives 4.0 International License, which permits any non-commercial use, sharing, distribution and reproduction in any medium or format, as long as you give appropriate credit to the original author(s) and the source, provide a link to the Creative Commons licence, and indicate if you modified the licensed material. You do not have permission under this licence to share adapted material derived from this article or parts of it. The images or other third party material in this article are included in the article's Creative Commons licence, unless indicated otherwise in a credit line to the material. If material is not included in the article's Creative Commons licence and your intended use is not permitted by statutory regulation or exceeds the permitted use, you will need to obtain permission directly from the copyright holder. To view a copy of this licence, visit <http://creativecommons.org/licenses/by-nc-nd/4.0/>.

© The Author(s) 2025